Theory and Simulations of Parallel Electric Fields in Nonlinear Magnetosonic Waves: Two-Component Plasma

Yukiharu OHSAWA and Seiichi TAKAHASHI

Department of Physics, Nagoya University, Nagoya 464-8602, Japan

(Received: 29 August 2008 / Accepted: 26 November 2008)

The electric field parallel to the magnetic field, $E_\parallel$, in nonlinear magnetosonic waves is studied with theory and simulations. Both $E_\parallel$ and its integral along the magnetic field, $F = -\int E_\parallel ds$, are obtained analytically for small-amplitude ($\epsilon \ll 1$) waves. The magnitude of eF is proportional to $\epsilon \Gamma_e T_e$ in warm plasmas, where Γ_e is the specific heat ratio of electrons, and to $\epsilon^2 m_i v_{\rm A}^2$ in cold plasmas. These are verified with fully kinetic, electromagnetic, particle simulations. Furthermore, it is found that in large-amplitude waves [$\epsilon \sim O(1)$], $eF \sim \epsilon(m_i v_{\rm A}^2 + T_e)$ in both warm and cold plasmas.

Keywords: parallel electric field, magnetosonic wave, shock wave, particle simulation, collisionless plasma

1. Introduction

The electric field parallel to the magnetic field is zero, $E_\parallel = 0$, in the ideal magnetohydrodynamics (MHD). It is thus generally thought that the parallel electric field is quite weak in MHD phenomena. In some simulations [1, 2], however, the parallel electric field in a magnetosonic shock wave has been found to be quite strong; in other words, the integral of $E_\parallel$ along the magnetic field, which is referred to as the parallel pseudo potential and is denoted by F, is quite large, $eF \sim m_e c^2$, where m_e is the electron mass and c is the speed of light.

In this paper, we study the parallel electric field and parallel pseudo potential with theory and fully kinetic, electromagnetic, particle simulations.

In Sec. 2, we describe the theory for $E_\parallel$ and F in nonlinear magnetosonic waves. In the theory based on the conventional perturbation scheme, the parallel electric field appears in the lowest-order perturbation, and the parallel pseudo potential is found to be proportional to the electron temperature, $eF \sim \epsilon \Gamma_e T_e$, where ϵ is the wave amplitude, and Γ_e is the specific heat ratio of electrons. For the cold plasma, for which the above theory gives $F = 0$, we calculate up to the second-order quantities and find that $eF \sim \epsilon^2 m_i v_{\rm A}^2$, where $v_{\rm A}$ is the Alfvén speed. That is, in low beta plasmas, where beta is the ratio of kinetic to magnetic pressures, the parallel pseudo potential is proportional to ϵ^2 and to the energy density of the external magnetic field [3].

In Sec. 3, we examine these predictions with one-dimensional, electromagnetic, particle simulations. By generating small-amplitude, magnetosonic, solitary pulses and measuring the field strengths in them, we verify the above predictions. Furthermore, we investigate the large-amplitude case with $\epsilon \sim O(1)$, i.e., shock waves. The simulation values of the parallel pseudo potential fit fairly well to the phenomenological relation $eF \sim \epsilon(m_i v_{\rm A}^2 + \Gamma_e T_e)$ in both high and low beta cases.

These results indicate that the parallel electric field can be quite strong in intense magnetic fields, such as in solar magnetic tubes and around pulsars. We summarize our work in Sec. 4.

2. Theory for Parallel Electric Field

Here, we consider one-dimensional magnetosonic waves propagating in the x direction ($\partial/\partial y = \partial/\partial z = 0$) in an external magnetic field $\boldsymbol{B}_0 = B_0(\cos\theta, 0, \sin\theta)$. By integrating the parallel electric field,

$$\boldsymbol{E}_\parallel = \frac{(\boldsymbol{E}\cdot\boldsymbol{B})\boldsymbol{B}}{B^2}, \tag{1}$$

along the magnetic field, we define the quantity F as

$$F = -\int E_\parallel ds, \tag{2}$$

where s is the length along the magnetic field. Since $E_\parallel$ contains longitudinal and transverse electric fields, we call this quantity the parallel pseudo potential. (Note that the electric potential ϕ is the integral of the longitudinal electric field E_x along x.)

2.1 Warm Plasma

With use of the conventional reductive perturbation method [4, 5], the parallel electric field and parallel pseudo potential in a warm plasma is obtained as [3]

$$E_\parallel = -\frac{\Gamma_e T_e}{e}\frac{\partial}{\partial s}\left(\frac{n_1}{n_0}\right), \tag{3}$$

$$eF_T = \Gamma_e T_e \frac{n_1}{n_0}, \tag{4}$$

author's e-mail: ohsawa@nagoya-u.jp

where n_0 and n_1 are, respectively, the equilibrium and perturbed electron densities (the subscript 1 refers to the first-order quantities). Since the parallel pseudo potential is proprotional to T_e, we have used the subscript T for F in warm plasmas. The magnetic perturbation B_{z1} is related to n_1 as

$$\frac{B_{z1}}{B_0} = \frac{(v_{p0}^2 - c_s^2)}{v_{\rm A}^2 \sin\theta}\frac{n_1}{n_0}, \tag{5}$$

where v_{p0} is the phase velocity ω/k of the magnetosonic wave in the long-wavelength limit, and c_s is the sound speed. The expression for the parallel pseudo potential in magnetosonic waves, Eq. (4), is analogous to that for the potential ϕ in ion-acoustic waves in the absence of external magnetic field.

It is noted that the effect of the magnetic field does not appear in Eq. (4), even though the magnetosonic wave has a large electric potential, the magnitude of which is

$$e\phi_1 \simeq m_i \left(v_{\rm A}^2 + \frac{\Gamma_e p_{e0}}{n_0(m_i + m_e)} \right) \frac{B_{z1}}{B_0}, \tag{6}$$

in quasi-perpendicular waves with $\sin\theta \simeq 1$. The effect of the magnetic field appears in both E_x and E_z. Even though the terms due to the magnetic field are not small, they cancel in the lowest-order calculation of $E_\parallel$,

$$E_\parallel = \frac{E_{x1}B_{x0} + E_{z1}B_{z0}}{B_0}, \tag{7}$$

and only the terms arising from the electron pressure remain, as shown in Eq. (4).

2.2 Cold Plasma

According to Eqs. (3) and (4), $E_\parallel$ and F become zero in a cold plasma ($T = 0$). Some simulations have shown, however, that F can be quite large ($eF \gtrsim m_e c^2$) even when the plasma beta value is much smaller than unity [1, 2].

To obtain the parallel electric field in a cold plasma, we calculate higher order terms. The parallel electric field including up to the second-order terms may be written as

$$\begin{aligned} E_\parallel &= \frac{\boldsymbol{E}_1 \cdot \boldsymbol{B}_0}{B_0}\left(1 - \frac{\boldsymbol{B}_1 \cdot \boldsymbol{B}_0}{B_0^2}\right) \\ &+ \frac{\boldsymbol{E}_1 \cdot \boldsymbol{B}_1}{B_0} + \frac{\boldsymbol{E}_2 \cdot \boldsymbol{B}_0}{B_0}. \end{aligned} \tag{8}$$

Calculations show that the term $\boldsymbol{E}_1 \cdot \boldsymbol{B}_1 = E_{y1}B_{y1} + E_{z1}B_{z1}$ vanishes in both warm and cold plasmas, and the term $\boldsymbol{E}_1 \cdot \boldsymbol{B}_0/B_0$ is zero in cold plasmas. We can write $\boldsymbol{E}_2 \cdot \boldsymbol{B}_0/B_0$ with first-order quantities and find that

$$E_\parallel = \frac{m_i v_{\rm A}^2}{e}\cos\theta \left(\frac{c}{\omega_{pe}}\right)^2 \frac{\partial^3}{\partial \xi^3}\frac{B_{z1}}{B_0}, \tag{9}$$

$$eF_B = -m_i v_{\rm A}^2 \left(\frac{c}{\omega_{pe}}\right)^2 \frac{\partial^2}{\partial \xi^2}\frac{B_{z1}}{B_0}, \tag{10}$$

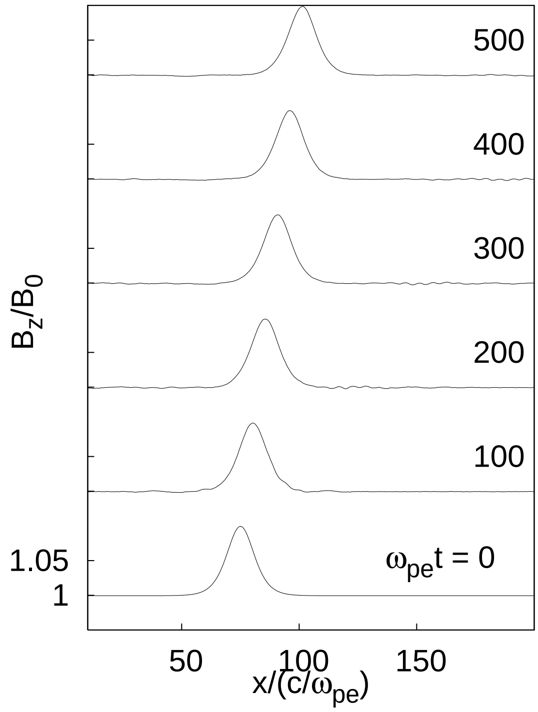

Fig. 1 B_z profiles of a solitary pulse with $\theta = 88°$.

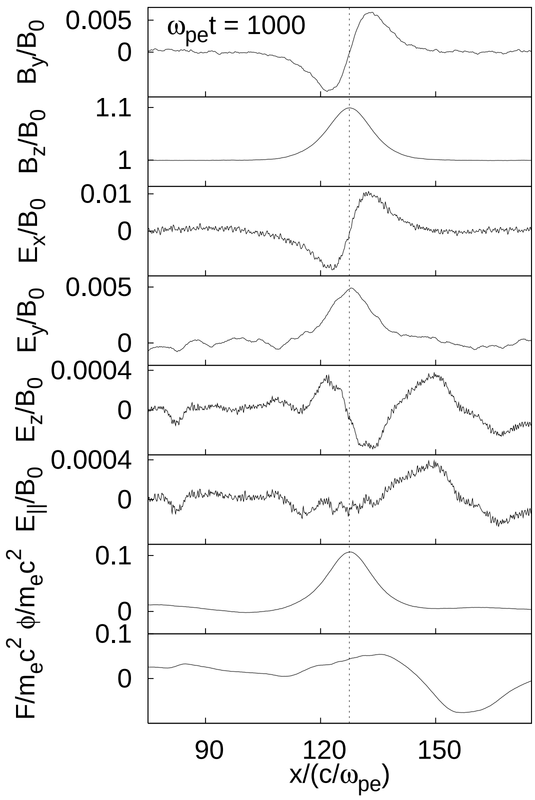

Fig. 2 Snapshot of field profiles at $\omega_{pe}t = 1000$. The profiles of E_z, $E_\parallel$, and F are vague compared with other field profiles.

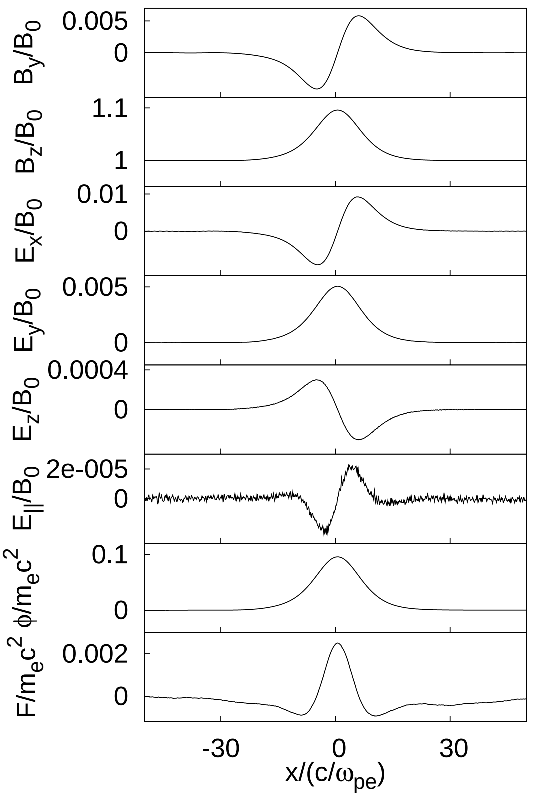

Fig. 3 Time-averaged field profiles. The profiles of E_z, $E_\parallel$, and F are also found to be consistent with the profiles predicted by the theory.

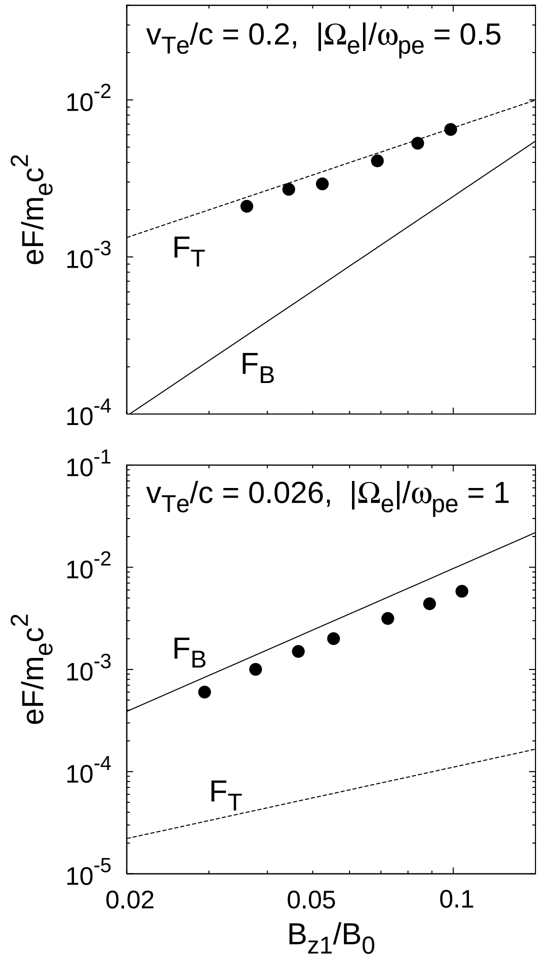

Fig. 4 Parallel pseudo potential F versus amplitude B_{z1}/B_0 for small-amplitude solitary pulses. In the high beta case (upper panel), the magnitude of F_T, which is for warm plasmas, is much greater than that for cold plasmas, F_B. The simulation results (dots) fit to the theory F_T. In the low beta case (lower panel), $F_B > F_T$, and the simulation results fit to the theoretical line of F_B.

where ξ is the stretched coordinate defined as [4, 5]

$$\xi = \epsilon^{1/2}(x - v_{p0}t). \tag{11}$$

Since F is determined by the magnetic field, we have used the subscript B for F in cold plasmas. These are the expressions for quasi-perpendicular waves; i.e., we have used the approximation $\sin\theta \simeq 1$ [accurate up to the first order of $(\pi/2 - \theta)$].

From Eqs. (4) and (10), we see that the parallel pseudo potential F is proportional to ϵT_e in warm plasmas and to $\epsilon^2 B_0^2$ in cold plasmas.

3. Results of Particle Simulations

We now examine the parallel electric field with one-dimensional (one space coordinate and three velocities), fully kinetic, relativistic, electromagnetic particle simulations. In the simulations, we generate magnetosonic solitary waves or shock waves and observe their propagation.

The simulation parameters are as follows: The system size is $L = 2048\Delta_{\rm g}$, where $\Delta_{\rm g}$ is the grid spacing. The numbers of simulation particles are $N_i = N_e \simeq 2.5 \times 10^6$. The ion-to-electron mass ratio is $m_i/m_e = 400$; hence, the critical angle [5], at which the dispersion of the magnetosonic wave disappears (ω is proportional to k), is $\theta_c = 87.1°$. The speed of light is $c/(\omega_{pe}\Delta_{\rm g}) = 10$. The ion thermal speed is fixed to be $(T_i/m_i)^{1/2}/(\omega_{pe}\Delta_{\rm g}) = 0.013$. The time step is $\omega_{pe}\Delta t = 0.05$.

Figure 1 shows the profiles of B_z of a solitary pulse excited in a simulation. From the profiles of $B_z(x, t_j)$ at consecutive times t_j $(j = 1, 2, \cdots, N)$, we can obtain the propagation speed $v_{\rm sh}$ of the pulse.

The parallel electric field $E_\parallel$ is weaker than E_x and E_y, and F is smaller than the electric potential ϕ. They ($E_\parallel$ and F) therefore tend to be easily masked by thermal noise. To measure the amplitude and profile of, for instance, F in a small-amplitude pulse, we average the profiles of $F(x - v_{\rm sh}t_j, t_j)$ over time:

$$\langle F \rangle = \frac{1}{N}\sum_{j=1}^{N} F(x - v_{\rm sh}t_j, t_j). \tag{12}$$

This procedure smoothes out thermal fluctuations, and we find the profile of F.

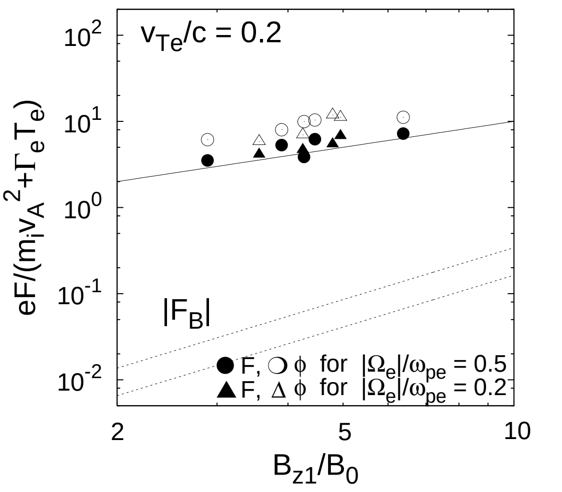

Fig. 5 Parallel pseudo potential F versus amplitude B_{z1}/B_0 for shock waves. In both high and low beta cases, the simulation results of F (closed circles and triangles) fit to the line given by Eq. (13). The magnitudes of F are comparable to those of ϕ (open circles and traiangles), even though $F < \phi$.

Figure 2 shows the snapshot of the field profiles of the pulse at $\omega_{pe}t = 1000$. The profiles of B_y, B_z, E_x, E_y, and ϕ are clear and are consistent with the ones predicted by the theory. The profiles of E_z, $E_\parallel$, and F are, however, rather vague, owing to the thermal noise.

If we perform the above averaging procedure on each field component, we obtain smooth field profiles, as shown in Fig. 3, from which we see that the profiles of E_z, $E_\parallel$, and F are also consistent with the theory. We can thus measure these quantities.

In Fig. 4 we plot the magnitude of F as a function of the pulse amplitude B_{z1}/B_0; the propagation angle is $\theta = 88°$ for both the upper and lower panels. The upper panel shows a high beta case ($v_{Te}/c = 0.2$ and $|\Omega_e|/\omega_{pe} = 0.5$), where $F_T > F_B$, and the simulation results (dots) fit well to the theoretical line of F_T. The lower panel shows a low beta case ($v_{Te}/c = 0.026$ and $|\Omega_e|/\omega_{pe} = 1$), where $F_B > F_T$, and the simulation results are explained by the theoretical line of F_B.

The above theory and simulation results are for small-amplitude waves. In large-amplitude pulses (shock waves), the parallel pseudo potential becomes quite large. We show in Fig. 5 the magnitude of F in shock waves; here, the propagation angle is $\theta = 60°$, and the electron thermal speed is $v_{Te}/c = 0.2$. The circles and triangles represent the simulation results for $|\Omega_e|/\omega_{pe} = 0.5$ and for $|\Omega_e|/\omega_{pe} = 0.2$, respectively. It is interesting to note that the values of F (closed circles and triangles) are close to the line given by the phenomenological relation

$$eF \sim (m_i v_{\rm A}^2 + \Gamma_e T_e)\frac{B_{z1}}{B_0}. \tag{13}$$

Another important point is that F is comparable to ϕ. (The relation $F < \phi$, however, still holds). This differs from the small-amplitude case, in which F is much smaller than ϕ especially in low beta plasmas.

4. Summary

We have studied the parallel electric field in nonlinear magnetosonic waves with theory and particle simulations. Our results show that the parallel electric field can be strong even in magnetohydrodynamic phenomena in high-temperature plasmas.

The theory for small-amplitude waves predicts that the magnitude of parallel pseudo potential is $eF \sim \epsilon\Gamma_e T_e$ in warm plasmas and is $eF \sim \epsilon^2 m_i v_{\rm A}^2$ in cold plasmas. These predictions have been verified with one-dimensional, fully kinetic, electromagnetic particle simulations.

Large-amplitude waves (shock waves) have also been investigated with simulations. It has been shown that the phenomenological relation $eF \sim \epsilon(m_i v_{\rm A}^2 + \Gamma_e T_e)$ explains the simulation results for both warm and cold plasmas.

[1] N. Bessho and Y. Ohsawa, Phys. Plasmas **6**, 3076 (1999); *ibid.* **9**, 979 (2002)..
[2] H. Hasegawa, K. Kato, and Y. Ohsawa, Phys. Plasmas **12**, 082306 (2005).
[3] S. Takahashi and Y. Ohsawa, Phys. Plasmas **14**, 112305 (2007).
[4] T. Taniuti and C. C. Wei, J. Phys. Soc. Jpn. **24**, 941 (1968).
[5] T. Kakutani, H. Ono, T. Taniuti, and C. C. Wei, J. Phys. Soc. Jpn. **24**, 1159 (1968).